

The Nuclear Response in Delta-Isobar Region
in the ($^3\text{He},t$) Reaction

V.F.Dmitriev

Nuclear Theory Center, Indiana University, Bloomington IN 47408

and

Budker Institute of Nuclear Physics, Novosibirsk, 630090, Russia

The excitation of a Δ -isobar in a finite nucleus in charge-exchange ($^3\text{He},t$) reaction is discussed in terms of a nuclear response function. The medium effects modifying a Δ - and a pion propagation were considered for a finite size nucleus. The Glauber approach has been used for distortion of a ^3He and a triton in the initial and the final states. The effects determining the peak positions and its width are discussed. Large displacement width for the Δ - h excitations and considerable contribution of coherent pion production were found for the reaction on ^{12}C .

I. INTRODUCTION

The experimental studies of nuclear response in charge-exchange reactions were extended in the eighties to high excitation energies where a first nucleon resonance the Δ -isobar can be excited [1]. The detailed studies were done for the (${}^3\text{He},t$) charge-exchange reaction at different projectile energies [2] and different targets [3]. The properties of the Δ excited in a nucleus were found different compared to the case of the reaction on a single nucleon. The difference was both in the peak position and the width of the resonance excited in a complex nucleus. The review of the observed phenomena can be found in the recent paper [4].

The appealing explanation of this phenomenon is related to medium effects, namely, the excitation of a pionic nuclear mode [5], [6], [7], [8] although another explanation has been proposed as well [9]. In this picture the Δ in nuclear matter does not exist as separate resonance but forms a collective excitation consisting of pionic, Δ and nucleon degrees of freedom.

At first sight one should not expect sizeable medium effects for (${}^3\text{He},t$) reaction since the reaction takes place at the surface of the target [10]. For inelastic reactions, however, the absorption is smaller and one should use absorption factor different from that used for elastic scattering [11] providing both the medium effects and the magnitude of inelastic cross-section. Another important point is the account of the finite target size in the response function. As it will be shown below different Δ -hole multipoles are peaked at different energies so, part of the observed width can be attributed to this displacement. Besides, on finite nucleus the process of coherent pion production is possible. The process is absent in infinite nuclear matter and it contributes to the shift of the peak position as well.

Here we present the results of the absolute cross-section calculations of the ${}^{12}\text{C}({}^3\text{He},t)$ reaction at 0° and at the kinetic energy of the ${}^3\text{He}$ $T_{He}=2$ GeV. In the next section we discuss the model for the reaction amplitude that is a driving force for the nuclear response. In the section IV the pionic response function of a finite nucleus is discussed and the cross-section is calculated in the section VI.

II. REACTION AMPLITUDE.

We shall start from the discussion of the models for the elementary charge-exchange reaction $p(p,n)\Delta^{++}$. From the early sixties it was shown this reaction can be described by OPE model [12], at least at low momentum transfer. This analysis has been extended for wide range of the proton energies in [13], and has been repeated with some minor modifications in connection to the analysis of $p(^3\text{He},t)\Delta^{++}$ reaction in [14]. As it was shown all existing data in the region of low momentum transfer are well described by OPE with the soft monopole πNN - and $\pi N\Delta$ - form factors

$$F(q^2) = \frac{\Lambda^2 - \mu^2}{\Lambda^2 - q^2} \quad (1)$$

The parameter $\Lambda = 650$ MeV at low proton energy and slightly decreases with the proton energy reflecting increase of the absorption effects at high energy. With these soft form factors (1) the main contribution to the Δ -production comes from the direct graph shown in Fig.1. The exchange contribution is small for the $p(p,n)\Delta^{++}$ reaction.

In this model the amplitude is completely longitudinal with respect to the momentum transfer. In the other model used for the description of the Δ - production at 800 MeV proton energy [15] the transverse part of the amplitude was described by ρ - exchange and hard form factors with $\Lambda = 1.2$ GeV and $\Lambda = 1.7$ GeV were used for $\pi N\Delta$ - and $\rho N\Delta$ - vertexes. The magnitude of the cross-section and the momentum transfer dependence are reproduced in this model due to cancellation between the direct and the exchange parts of the amplitude. The cancellation is rather delicate and at higher proton energy it can be broken resulting in wrong momentum transfer dependence [14].

At very high energy the situation is different. The π -exchange contribution decreases as s^{-2} , where s is the center-of-mass energy squared, while for the ρ -exchange the decrease is slower. Its contribution falls down like $s^{-2+\alpha(0)}$ for small momentum transfer where $\alpha(t)$ is the corresponding Regge-trajectory. Thus, in the asymptotic region at high energy one should expect the dominance of the ρ -exchange even at forward angles. Below 20 GeV

the cross-section for forward scattering follows the $1/s^2$ law [16] so, the contribution of ρ -exchange at intermediate energies is believed to be small.

For the $p(^3\text{He},t)\Delta^{++}$ reaction the situation is similar to the (p,n) case. The π -exchange with the soft form factors (1) gives reasonable description of the absolute cross-section and the tritium spectrum at forward angle for all existing data [14]. Nevertheless, at the kinetic energy of ^3He 2 GeV, which is close in kinematics to 800 MeV (p,n) one can get good description using $\pi + \rho$ - exchanges as well [17]. It would be very desirable to extend the last analysis to higher ^3He energies.

III. NUCLEAR MATTER RESPONSE TO THE PIONIC PROBE.

A. ($^3\text{He},t$) Cross-Section in Plane Wave Approximation.

It is convenient to start with the plane waves for both projectile and ejectile in order to obtain an expression for the cross-section that can be easily generalized to the distorted waves. In PWIA the cross-section is proportional to the matrix element, shown in Fig.1, squared and summed over final nuclear and Δ - states.

$$T = \int d^3r \Gamma_{\pi H e t}(\mathbf{r}) \cdot G_0(\mathbf{r} - \mathbf{r}') \cdot \Gamma_{\pi N \Delta}(\mathbf{r}') d^3r' \quad (2)$$

For plane waves $\Gamma \sim \exp(i\mathbf{q}\mathbf{r})$, it gives for the cross-section

$$\frac{d^2\sigma}{dE'd\Omega} = \frac{M_{He}^2 p'}{4\pi^2 p} \overline{|\Gamma_{\pi H e t}(\mathbf{q})|^2} \sum_{\Delta h} \delta(\omega - E_{\Delta h}) n_h |\Gamma_{\pi N \Delta}(\mathbf{q})|^2 \cdot |G_0(q)|^2 \quad (3)$$

The expression under the sum is just imaginary part of the pionic self-energy in nuclear medium.

$$\Im m \Pi_{\Delta}(\omega, \mathbf{q}, \mathbf{q}) = \pi \sum_{\Delta h} \delta(\omega - E_{\Delta h}) |\Gamma_{\pi N \Delta}|^2 n_h \quad (4)$$

Using the pionic self-energy (4) we obtain the final expression for the cross-section suitable for inclusion of medium effects.

$$\frac{d^2\sigma}{dE'd\Omega} = \frac{M_{He}^2 p'}{4\pi^3 p} \overline{|\Gamma_{\pi H e t}(\mathbf{q})|^2} G_0^*(q) \cdot \Im m \Pi_{\Delta}(\omega, \mathbf{q}, \mathbf{q}) \cdot G_0(q). \quad (5)$$

B. Medium Effects in Nuclear Matter

The main effect of nuclear medium is the renormalization of the pion propagator by intermediate Δ -hole loops giving the major contribution to the pionic self-energy (4) near the Δ -resonance. To take it into account one must change in (5) the bare pion propagator $G_0(q)$ for the dressed one $G(\omega, \mathbf{q})$, where

$$G(\omega, \mathbf{q}) = \frac{1}{q^2 - \mu^2 - \Pi_\Delta(\omega, \mathbf{q})}.$$

Making this change we are going out of the scope of the impulse approximation.

The imaginary part of the bare pion propagator is equal to zero for negative q^2 . Using it we obtain $G^*(\omega, \mathbf{q}) \cdot \Im m \Pi_\Delta(\omega, \mathbf{q}) \cdot G(\omega, \mathbf{q}) = -\Im m G(\omega, \mathbf{q})$. With these changes the cross-section (5) becomes

$$\frac{d^2\sigma}{dE'd\Omega} = -\frac{M_{He}^2}{4\pi^3} \frac{p'}{p} \frac{1}{|\Gamma_{\pi Het}(\mathbf{q})|^2} \cdot \Im m G(\omega, \mathbf{q}). \quad (6)$$

It is clear from (6) the pion propagator $G(\omega, \mathbf{q})$ in nuclear medium is just the response function to a virtual pion probe. The excitation created by a virtual pion is no more pure Δ -hole but a superposition of the Δ -hole and pionic degrees of freedom, which is usually called the pionic mode.

The unquenched Δ -hole self-energy (4) produces too much of attraction giving unreasonably low excitation energy for the pionic mode. In order to make the description more accurate several effects should be taken into account. First of all, more correct πN - scattering amplitude reproducing $s_{\frac{1}{2}}$ and $p_{\frac{1}{2}}$ partial waves should be used since we are interested in the energies lower than the Δ in vacuum. For this purpose one should add the Born diagrams with a nucleon intermediate state, u -channel Δ diagram and a σ -term arising from the σ -commutator [18]. Second, the short-range $N\Delta$ - correlations must be taken into account.

$$W(\mathbf{r}_1, \mathbf{r}_2) = \frac{f_\Delta^2}{\mu^2} g'_\Delta (\mathbf{S}_1^\dagger \cdot \mathbf{S}_2) (\mathbf{T}_1^\dagger \cdot \mathbf{T}_2) \delta(\mathbf{r}_1 - \mathbf{r}_2). \quad (7)$$

In nuclear matter the effect of short-range correlations can be accounted in the following

way. Let us define the Δ -hole response function $\chi(\omega, \mathbf{q})$ by

$$\Pi_{\Delta}(\omega, \mathbf{q}) = \left(\frac{\Lambda^2 - \mu^2}{\Lambda^2 - q^2} \right)^2 \mathbf{q}^2 \cdot \chi(\omega, \mathbf{q}).$$

Then,

$$\tilde{\Pi}_{\Delta}(\omega, \mathbf{q}) = \frac{\Pi_{\Delta}(\omega, \mathbf{q})}{1 - g'_{\Delta} \cdot \chi(\omega, \mathbf{q})}. \quad (8)$$

Similar effect should be taken into account for the nucleon-hole response function as well. But, in the region of interest in excitation energy its contribution is negligible and will be omitted below. In contrast, the backward Δ -hole loops and the σ -term must be retained since they have their own dependence on the virtual pion mass $-q^2$ that influences the position of the pionic branch in nuclear matter.

Finally, the virtual pion can be absorbed in nuclear medium emitting two or more nucleons. In the resonance region the absorption goes via intermediate Δ and it can be described by a Δ -nucleus optical potential. At lower energies the other mechanisms with different intermediate states contribute to the absorption. To take it into account we use the Ericson-Ericson optical potential from pionic atoms [19]

$$V_{2N} = -4\pi i ImC \cdot n^2(r) \cdot \mathbf{q}^2,$$

where $n(r)$ is the nuclear matter density. For pionic atoms $ImC = 0.08 \cdot \left(\frac{\hbar}{\mu c}\right)^6$. It was obtained from the fit of the mesoatomic level width and contains all absorption mechanisms including the intermediate Δ . Using this value in our case will give double counting since intermediate Δ is considered explicitly. Thus, ImC should be considered as a free parameter accounting another absorption mechanisms.

With these corrections the pion self-energy in nuclear matter is

$$\Pi(\omega, \mathbf{q}) = \tilde{\Pi}_{\Delta}(\omega, \mathbf{q}) + \frac{1}{f_{\pi}^2} \left(1 - \frac{2q^2}{\mu^2} \right) \sigma(0) \cdot n(r) + V_{2N}, \quad (9)$$

where f_{π} is the pion decay constant $f_{\pi} = 133$ MeV and $\sigma(0)$ is the σ -commutator for forward pion scattering. $\tilde{\Pi}_{\Delta}(\omega, \mathbf{q})$ includes both forward and backward Δ -hole loops corrected for short-range correlations.

IV. RESPONSE FUNCTION OF A FINITE NUCLEUS.

For a finite nucleus it is convenient to work in the configuration space where the self-energy (9) and the pion propagator become the functions of two distinct variables instead of functions of the distance between coordinate points in nuclear matter.

$$\Pi(\omega, \mathbf{r} - \mathbf{r}') \rightarrow \Pi(\omega, \mathbf{r}, \mathbf{r}');$$

$$V_{2N} = 4\pi i \text{Im} C (\nabla \cdot n^2(r) \cdot \nabla) \delta(\mathbf{r} - \mathbf{r}').$$

The $\pi N\Delta$ - vertex in the configuration space is

$$\Gamma_{\pi N\Delta}(\mathbf{r}, \mathbf{r}') = -i \mathbf{T}(\mathbf{S} \cdot \nabla) \frac{f_\Delta}{\mu} \frac{\Lambda^2 - \mu^2}{4\pi} \frac{\exp(-\kappa |\mathbf{r} - \mathbf{r}'|)}{|\mathbf{r} - \mathbf{r}'|}, \quad (10)$$

where $\kappa^2 = \Lambda^2 - \omega^2$.

A. Multipole Expansion

For a spherical nucleus the self-energy (9) has simple multipole expansion

$$\Pi(\omega, \mathbf{r}, \mathbf{r}') = \sum_{JM} \Pi_J(r, r') Y_{JM}^*(\mathbf{n}) Y_{JM}(\mathbf{n}').$$

The similar expansion exists for the $\pi N\Delta$ -vertex

$$\Gamma_{\pi N\Delta}(\mathbf{r} - \mathbf{r}') = \sum_{JLM} \Gamma_{JL}^0(r, r') Y_{JM}^*(\mathbf{n}) T_{JM}^L(\mathbf{n}'), \quad (11)$$

where the tensor operator

$$T_{JM}^L(\mathbf{n}') = \mathbf{S} \cdot \mathbf{Y}_{JM}^L(\mathbf{n}) = [\mathbf{S} \wedge Y_{Lm}(\mathbf{n})]_{JM}, \quad (12)$$

and the radial vertex $\Gamma_{JL}^0(r, r')$ is

$$\Gamma_{JL}^0(r, r') = i(L - J) \frac{f_\Delta}{\mu} \frac{2\kappa^2(\Lambda^2 - \mu^2)}{\pi} \sqrt{\frac{J + L + 1}{2(2J + 1)}} \begin{cases} i_L(\kappa r) k_J(\kappa r') & \text{if } r < r', \\ -i_J(\kappa r') k_L(\kappa r) & \text{if } r > r', \end{cases} \quad (13)$$

here $i_L(x)$ and $k_L(x)$ are the spherical Bessel functions with an imaginary argument. This is the advantage of using the simple scalar formfactors (1).

The Δ -hole response function χ can be expanded using the set of tensor operators (12)

$$\begin{aligned} \chi_{LL'}^J(r, r') &= \frac{1}{2J+1} \sum_{j_N l_N} \langle j_N l_N \| T_J^L \| j_{\Delta} l_{\Delta} \rangle \langle j_{\Delta} l_{\Delta} \| T_J^{L'} \| j_N l_N \rangle [g_{j_{\Delta} l_{\Delta}}(\omega + \epsilon_{j_N l_N}; r, r') \\ &+ g_{j_{\Delta} l_{\Delta}}(-\omega + \epsilon_{j_N l_N}; r, r')] \cdot n_{j_N l_N} \cdot R_{j_N l_N}(r) R_{j_N l_N}(r'), \end{aligned} \quad (14)$$

where $n_{j_N l_N}$ are the nucleon occupation numbers, $R_{j_N l_N}(r)$ the radial wave function of bounded nucleon and the $\epsilon_{j_N l_N}$ is its energy. $g_{j_{\Delta} l_{\Delta}}(\omega; r, r')$ is the Green function of the radial Schrödinger equation for the Δ moving in the mean nuclear optical potential. It was calculated using two independent solutions of the radial Schrödinger equation.

The Δ -hole contribution to the pion self-energy was calculated using the following expression

$$\tilde{\Pi}_{\Delta}^J(\omega; r, r') = \sum_{LL'} \int \rho^2 d\rho \rho'^2 d\rho' \Gamma_{JL}^0(r, \rho) \chi_{LL'}^J(\rho, \rho') \Gamma_{JL'}^*(\rho, r'); \quad (15)$$

where Γ_{JL} related to Γ_{JL}^0 via linear integral equation accounting the short-range correlations (7)

$$\Gamma_{JL}(r, \rho) = \Gamma_{JL}^0(r, \rho) + g' \left(\frac{f_{\Delta}}{\mu} \right)^2 \sum_{L'} \int \rho'^2 d\rho' \Gamma_{JL'}(r, \rho') \chi_{L'L}^J(\rho', \rho). \quad (16)$$

V. THE EFFECTS OF DISTORTION

For numerical calculations it is convenient to come back from expression (6) to more complex one similar to (5)

$$\frac{d^2\sigma}{dE'd\Omega} = \frac{M_{He}^2}{4\pi^2} \frac{p'}{p} \overline{\Gamma_{\pi Het}^{\dagger} \cdot G^* \cdot \Im m \Pi \cdot G \cdot \Gamma_{\pi Het}}. \quad (17)$$

The product sign means integration over all coordinates in the configuration space and the overline is the averaging and summing over spins of a ${}^3\text{He}$ and a triton.

In infinite matter (17) would be the only contribution to the inclusive cross-section. In finite nucleus, however, the cut of a bare pionic line gives nonzero contribution corresponding to coherent pion production.

$$\frac{d^2\sigma_c}{dE'd\Omega} = -\frac{M_{He}^2 p'}{4\pi^2 p} \overline{\Gamma_{\pi Het}^\dagger \cdot G^* \cdot \Pi^* \cdot \Im m G^0 \cdot \Pi \cdot G \cdot \Gamma_{\pi Het}}. \quad (18)$$

In the plane wave approximation the $\pi^3\text{Het}$ vertex is

$$\Gamma_{\pi Het}(\mathbf{r}) = \sqrt{2}(\boldsymbol{\sigma} \cdot \tilde{\mathbf{q}}) F(q^2) \frac{f_N(q^2)}{\mu} \exp(i\mathbf{q}\mathbf{r}), \quad (19)$$

where the effective momentum transfer $\tilde{\mathbf{q}}$ in lab. system is

$$\tilde{\mathbf{q}} = \sqrt{\frac{E' + M}{E + M}} \mathbf{p} - \sqrt{\frac{E + M}{E' + M}} \mathbf{p}',$$

here E is the total energy of ${}^3\text{He}$ and M is its mass. At first order in $\frac{\omega}{E+M}$ it can be rewritten as

$$\tilde{\mathbf{q}} = \mathbf{q} - \frac{1}{2} \frac{\omega}{E + M} (\mathbf{p} + \mathbf{p}')$$

The effective momentum transfer squared coincides with the four-momentum transfer squared. $F(q^2)$ is the (${}^3\text{He}, t$) transition form factor.

The multipole expansion of the vertex looks as follows

$$\Gamma_{\pi Het}(\mathbf{r}) = \sum_{JLM} \Gamma_{LJM}^N(r) t_{JM}^L(\mathbf{n}), \quad (20)$$

where $t_{JM}^L(\mathbf{n})$ are the tensor operators analogous to the (12)

$$t_{JM}^L(\mathbf{n}) = (\boldsymbol{\sigma} \cdot \mathbf{Y}_{JM}^L(\mathbf{n})) = [\boldsymbol{\sigma} \wedge Y_{LM}]_{JM}. \quad (21)$$

For plane waves the radial vertex is

$$\Gamma_{JLM}^{0N}(r) = \sqrt{2} (i)^L j_L(qr) [\tilde{\mathbf{q}} \wedge Y_{Lm}^*(\hat{\mathbf{q}})]_{JM} \frac{f_N(q^2)}{\mu} F(q^2) \quad (22)$$

The distortion of the incoming and outgoing waves has been taken into account via inelastic distortion factor [11]. With this factor the $\pi^3\text{Het}$ vertex becomes

$$\Gamma_{\pi Het}(\mathbf{r}) = \sqrt{2} [-i(\boldsymbol{\sigma} \cdot \nabla) - \frac{1}{2} \frac{\omega}{E + M} (\boldsymbol{\sigma} \cdot (\mathbf{p} + \mathbf{p}'))] \frac{f_N(q^2)}{\mu} \exp(i\mathbf{q}\mathbf{r}) \exp(-\frac{1}{2} \chi_{in}(\mathbf{r}_\perp, \mathbf{q})). \quad (23)$$

The distortion factor $\exp(-\frac{1}{2} \chi_{in}(\mathbf{r}_\perp, \mathbf{q}))$ is [11]

$$\begin{aligned} \exp\left(-\frac{1}{2}\chi_{in}(\mathbf{r}_\perp, \mathbf{q})\right) &= \left(1 - \frac{1}{A}\bar{\gamma}T(\mathbf{r}_\perp)\right)^{A-1} \cdot \int d^3s_1 d^3s_2 d^3s_3 \exp(i\mathbf{q}\mathbf{s}_1)\Psi^*(\mathbf{s}_1, \mathbf{s}_2, \mathbf{s}_3) \cdot \\ &\quad \left(1 - \frac{1}{A}\bar{\gamma}T(\mathbf{r}_\perp + \mathbf{s}_{2\perp} - \mathbf{s}_{1\perp})\right)^A \cdot \left(1 - \frac{1}{A}\bar{\gamma}T(\mathbf{r}_\perp + \mathbf{s}_{3\perp} - \mathbf{s}_{1\perp})\right)^A \cdot \\ &\quad \Psi(\mathbf{s}_1, \mathbf{s}_2, \mathbf{s}_3)\delta(\mathbf{s}_1 + \mathbf{s}_2 + \mathbf{s}_3), \end{aligned} \quad (24)$$

where $T(\mathbf{r}_\perp)$ is the thickness function

$$T(\mathbf{r}_\perp) = \int_{-\infty}^{\infty} \rho(\mathbf{r}_\perp, z) dz,$$

and $\rho(\mathbf{r}_\perp, z)$ is the target density. The

$$\bar{\gamma} = -i \frac{2\pi}{p_{lab}} f(0)$$

is related to the elastic nucleon–nucleon scattering amplitude at given energy per nucleon and $\Psi(\mathbf{s}_1, \mathbf{s}_2, \mathbf{s}_3)$ is the wave function of the ${}^3\text{He}$ or the triton depending on the internal coordinates \mathbf{s} . The value of $\bar{\gamma}$ used in calculations is $\bar{\gamma} = (2.1 - i0.26) fm^2$ [22].

Two features of the distortion factor (24) should be mentioned. First, the ${}^3\text{He}t$ form factor can not be separated from the effects of distortion. Second, since the vertex (23) has a gradient coupling and the distortion factor (24) depends on the transversal coordinates, some transversal components arise in the reaction amplitude even if it was before pure longitudinal amplitude.

The multipole expansion of the distorted vertex (23) can be obtained directly by multiplying it on $t_{JM}^{\dagger L}(\mathbf{n})$, taking trace over spin matrices, and integrating over angles of the unit radius vector \mathbf{n} .

$$\Gamma_{LJM}^N(r) = \frac{1}{2} Tr \int d\mathbf{n} \left(t_{JM}^{\dagger L}(\mathbf{n}) \cdot \Gamma_{\pi\text{Het}}(\mathbf{r}) \right). \quad (25)$$

The separate multipoles contribute independently into cross–section (17), which becomes

$$\frac{d^2\sigma}{dE'd\Omega} = \frac{M_{He}^2 p'}{4\pi^3 p} \sum_{LJM} \Gamma_{LJM}^{*N} \cdot G_L^* \cdot \Im m \Pi_L \cdot G_L \cdot \Gamma_{LJM}^N. \quad (26)$$

Similar expansion exist for the coherent pion contribution (18).

For numerical calculation it is convenient to define the function

$$w_{LJM}(r) = \int_0^\infty r'^2 dr' G_L(r, r') \Gamma_{LJM}^N(r'),$$

which is the pion field at the reaction point generated by the source $\Gamma_{LJM}^N(r')$. The integration in (V) is not well defined numerically since the integrand is oscillating function that is not decreasing at infinity. The indirect integration has been done in the following way. The function $w_{LJM}(r)$ satisfies the integro-differential equation

$$\int_0^\infty r'^2 dr' G_L^{-1}(r, r') w_{LJM}(r') = \Gamma_{LJM}^N(r), \quad (27)$$

which was solved numerically using the condition for Feynman propagator $G_L(r, r') = G_L^{(+)}(r, r')$ at positive energy. Since $G_L^{(+)}(r, r')$ has an outgoing wave at infinity it fixes the solution of the equation (27). The cross-section expressed in terms of $w_{LJM}(r)$ is

$$\frac{d^2\sigma}{dE'd\Omega} = \frac{M_{He}^2 p'}{4\pi^3 p} \sum_{LJM} w_{LJM}^* \cdot (\Im \Pi_L - \Pi_L^* \cdot \Im G^0 \cdot \Pi_L) \cdot w_{LJM}. \quad (28)$$

In the expression (28) the integration over coordinates goes effectively in a finite range, inside the target nucleus.

VI. THE TRITON SPECTRA FOR $^{12}\text{C}(^3\text{He}, T)$ REACTION AT 2 GEV

A. Parameters of the single-particle potentials.

The nucleon single-particle potential used for the wave functions of the bound nucleons has been taken in the standard Woods-Saxon form.

$$U(r) = V_0 \cdot f(r) + V_{LS} \frac{\lambda_\pi^2}{r} \frac{df(r)}{dr} (\sigma \cdot \mathbf{l}) + V_C(r),$$

where $f(r) = \frac{1}{1 + \exp(\frac{r-R}{a})}$, λ_π is the pion Compton wavelength, and $V_C(r)$ is the Coulomb potential for protons that was taken as the potential of a uniformly charged sphere. The parameters of the potential are listed in the Table 1. The response function (14) were found not very sensitive to the parameters of the nucleon potential.

The situation is, however, different for the optical Δ – nucleus potential that has been taken in similar Woods–Saxon form.

$$U_{\Delta}(r) = (V_{\Delta} + iW_{\Delta}) \cdot f(r) + (V_{\Delta LS} + iW_{\Delta LS}) \frac{\lambda_{\pi}^2}{r} \frac{df(r)}{dr} (\mathbf{s}_{\Delta} \cdot \mathbf{l}) + V_{\Delta C}(r),$$

where s_{Δ} are the spin 3/2 matrices. Fig. 2 shows two triton spectra for the Δ –h contribution demonstrating sensitivity to the real part of the Δ –nucleus optical potential. In the absence of the Δ –nucleus interaction the peak position coincides with the one in the reaction on free proton. The attraction produced by the real part of the potential in the final state increases cross-section and shifts the peak position on 15-20 MeV down. The parameters of the optical potential are listed in Table 2. They were taken mainly from [20], [21], and [7]. The radius R and the diffuseness a were kept the same as for the nucleons.

B. Medium Effects of Pion Renormalization

The main feature of the pionic self–energy near the resonance is its large imaginary part. It is instructive to study separately the effects of real and imaginary parts of the self–energy on the triton spectra. Fig.3 shows three spectra where either real or imaginary part of the self–energy were accounted in comparison to the quasifree case. The real part of the self–energy is attractive and it brings more strength to the Δ -hole peak. In analogy with particle–hole excitations one can say the real part of the pionic self–energy makes the Δ -hole peak more collective. The peak position, however, changes not much. The imaginary part, takes all this collectivity back decreasing cross–section due to incoherent Δ decay so, when both parts are taken into account the cross–section appeared close to its quasifree magnitude as it is shown in Fig.3 and Fig.4.

In Fig.3 one can see that the imaginary part of the self–energy produces also some shift in the peak position. The origin of the shift is, however, different from the shift due to the real part. To understand its origin let us return to nuclear matter and compare two expressions for the cross-sections with and without renormalization of the pion propagator.

Without renormalization the cross-section is proportional to

$$\frac{\Im m\Pi(\omega, \mathbf{q})}{(q^2 - \mu^2)^2},$$

while in the other case it is proportional to

$$\frac{\Im m\Pi(\omega, \mathbf{q})}{(q^2 - \mu^2)^2 + (\Im m\Pi(\omega, \mathbf{q}))^2}.$$

For simplicity the real part is omitted in this expression. The first case corresponds to quasifree mechanism and the peak position is at the same place as in the reaction on a proton. In the second case the cross-section starts to grow at the same threshold but at the resonance where $\Im m\Pi(\omega, \mathbf{q}) > (q^2 - \mu^2)$ we have the cross-section proportional to

$$\frac{1}{\Im m\Pi(\omega, \mathbf{q})}.$$

Thus, instead of maximum the cross-section appeared to be small at this energy. Since the cross-section is growing from threshold one can immediately conclude that the maximum of the cross-section will be below the resonance position. Fig.5 demonstrates this effect for the $L = 0$ multipole in the case of finite nucleus. This effect is not so much pronounced for higher multipoles that determine the magnitude of the cross-section. The higher multipoles undergo smaller medium effects since they are peaked at nuclear surface where the density is small. Therefore, the overall shift of the peak position is smaller than for $L = 0$. The imaginary part of the optical Δ - nucleus potential makes this effect stronger as it is shown in Fig.6.

C. Contribution of separate multipoles.

The contribution of separate multipoles to the triton spectrum is shown in the Fig.7. The contribution of the low multipoles $L = 0$ and $L = 1$ is almost negligible due to strong absorption of the incoming and outgoing ions. The main contribution comes from the multipoles between $L = 2$ to $L = 6$ although higher multipoles, at least up to $L = 10$, have to be considered at higher excitation energy.

Another feature clearly seen in the Fig.7 is rather wide spreading of the different multipole contributions. The $L = 2$ contribution is most sensitive to the medium effects shifting down the transition strength. It has the largest downward shift in the peak position. The absorption of the ${}^3\text{He}$ and t is smaller for $L = 2$ compared to $L = 0$ resulting in sizeable contribution to the cross-section. Higher multipoles have smaller medium effects and their peak positions are at more and more high excitation energies. This produce large displacement width of summed triton spectrum.

D. Coherent pion production.

Fig.8 shows the final triton spectrum together with separate contributions of the Δ -hole excitations and the coherent pion production. The process of coherent pion production gives sizeable contribution to the inclusive triton spectrum. The maximum of the cross-section is at about 240 MeV excitation energy and it also contributes to the shift of the inclusive peak. The coherent pion production is absent in infinite nuclear matter, therefore one should expect decrease of the relative yield of coherent pions for heavier nuclei.

VII. CONCLUSIONS

For (${}^3\text{He},t$) reaction in the Δ -region strong deviations from impulse approximations were demonstrated. The deviations come from the medium effects of renormalization of the pion propagator in the OPE mechanism of the elementary charge-exchange reaction. The medium effects change both the peak position and its height. Several effects, besides pion renormalization, contribute to the shift of peak position including Δ -nucleus optical potential, and coherent pion production. The possible effects of collectivity in the Δ -hole excitations are strongly suppressed by incoherent Δ decay. The effects of virtual pion propagation manifest itself only in the process of coherent pion production.

The finite size of a target nucleus produces together with the medium effects large spreading of the observed peak. The absorption in initial and final states strongly suppresses the

lowest multipoles of the angular momentum transfer. The Glauber approach to the distortion in initial and final states gives reasonable description both the size of the medium effects and the absolute value of the cross-section.

ACKNOWLEDGMENTS

During all stages of this work the discussions with Carl Gaarde and Thomas Sams were very stimulating and helpful. I would like to thank V.G.Zelevinsky and V.B.Telitsin as well for discussions of different aspects of the problem.

REFERENCES

- [1] C. Ellegaard et al., Phys. Rev. Lett. **50** (1983) 1745.
- [2] V.G. Ableev et al., JETP Lett. **40** (1984) 763.
- [3] D. Contardo et al., Phys. Lett. **168B** (1986) 331.
- [4] C. Gaarde, Annu. Rev. Nuc. Part. Sci., **41** (1991) 187.
- [5] G. Chanfray and M. Ericson, Phys. Lett. **141B** (1984) 163.
- [6] V.F. Dmitriev and Toru Suzuki, Nucl. Phys. **A438** (1985) 697. V.F. Dmitriev, Yad. Fiz. **46** (1987) 770.
- [7] S.W. Hong, F. Osterfeld and T. Udagawa, Phys. Lett. **245B** (1990) 1.
- [8] J. Delorm and P.A.M. Guichon, Phys. Lett. **263B** (1991) 157.
- [9] E. Oset, E. Shiino and H. Toki, Phys. Lett. **224B** (1989) 249.
- [10] H. Esbensen and T.-S.H. Lee, Phys. Rev. **C32** (1985) 1966.
- [11] V.F. Dmitriev, Phys. Lett. **226B** (1989) 219.
- [12] E. Ferrari, F. Selleri, Phys. Rev. Lett. **7** (1961) 387.
- [13] G. Wolf, Phys. Rev. **182** (1969) 1538.
- [14] V.F. Dmitriev, O.P. Sushkov and C. Gaarde, Nucl. Phys. **A459** (1986) 503.
- [15] B.J. Vervest, Phys. Lett. **83B** (1979) 161.
- [16] V.A. Karmanov et al., Sov. Journ. Nucl. Phys. **18** (1973) 1133.
- [17] P. Desgrolard, J. Delorme and C. Gignoux, preprint Inst. de Phys. Nucl. de Lyon, LYCEN 9205 (1992).
- [18] M.G. Olsson, E.T. Osypowsky, Nucl. Phys. **bf B101** (1975) 136.

- [19] M. Ericson and T.E.O. Ericson, *Ann. Phys.* **36** (1966) 323.
- [20] T.-S. H. Lee and K. Ohta, *Phys.Rev.* **C25** (1982) 3043.
- [21] J. H. Koch, E. J. Moniz and N. Ohtsuka, *Ann. of Phys.* **154** (1984) 99.
- [22] Stephen J. Wallace, in *Advances in Nuclear Physics*, Plenum Press, New York, Vol. 12, 1981.

TABLES

	$V_0(\text{MeV})$	$V_{LS}(\text{MeV})$	$R(\text{fm})$	$R_{LS}(\text{fm})$	$a(\text{fm})$	$a_{LS}(\text{fm})$
p	57	12	$1.25 \cdot A^{1/3}$	$1.25 \cdot A^{1/3}$	0.53	0.53
n	57	12	$1.25 \cdot A^{1/3}$	$1.25 \cdot A^{1/3}$	0.53	0.53

TABLE I. Parameters of the single-particle nucleon potential.

$V_\Delta(\text{MeV})$	$W_\Delta(\text{MeV})$	$V_{LS\Delta}(\text{MeV})$	$W_{LS\Delta}(\text{MeV})$
35	40	5	0

TABLE II. Parameters of the Δ - nucleus optical potential. The radius and diffuseness are the same as for the nucleons.

FIGURES

FIG. 1. Direct OPE graph for the Δ production.

FIG. 2. Quasifree Δ production. Dashed line - no Δ -nucleus potential. Solid line - $V_{\Delta} = -35$ MeV

FIG. 3. Effects of real and imaginary parts of the pion self-energy on the Δ -h part of the triton spectrum. Dotted line – no medium effects for pion. Dashed line – effect of the real part of the self-energy. Solid line – effect of the imaginary part of the pion self-energy.

FIG. 4. Dashed line – effect of the real part. Dotted line – effect of the imaginary part. Solid line – full pion self-energy included.

FIG. 5. The shift of the peak position due to imaginary part of the pion self-energy for $L = 0$ Δ -h multipole.

FIG. 6. Influence of the imaginary part of the Δ -nucleus optical potential. Dashed line $W_{\Delta} = 0$. Solid line $W_{\Delta} = 40$ MeV.

FIG. 7. Contribution of separate Δ -h multipoles.

FIG. 8. Different contributions to the triton spectrum. Dashed line – Δ -h contribution. Dotted line – coherent pion production. Solid line – full spectrum.

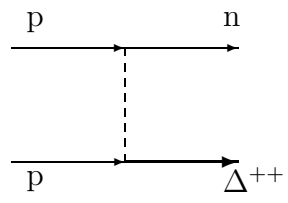


Fig.1

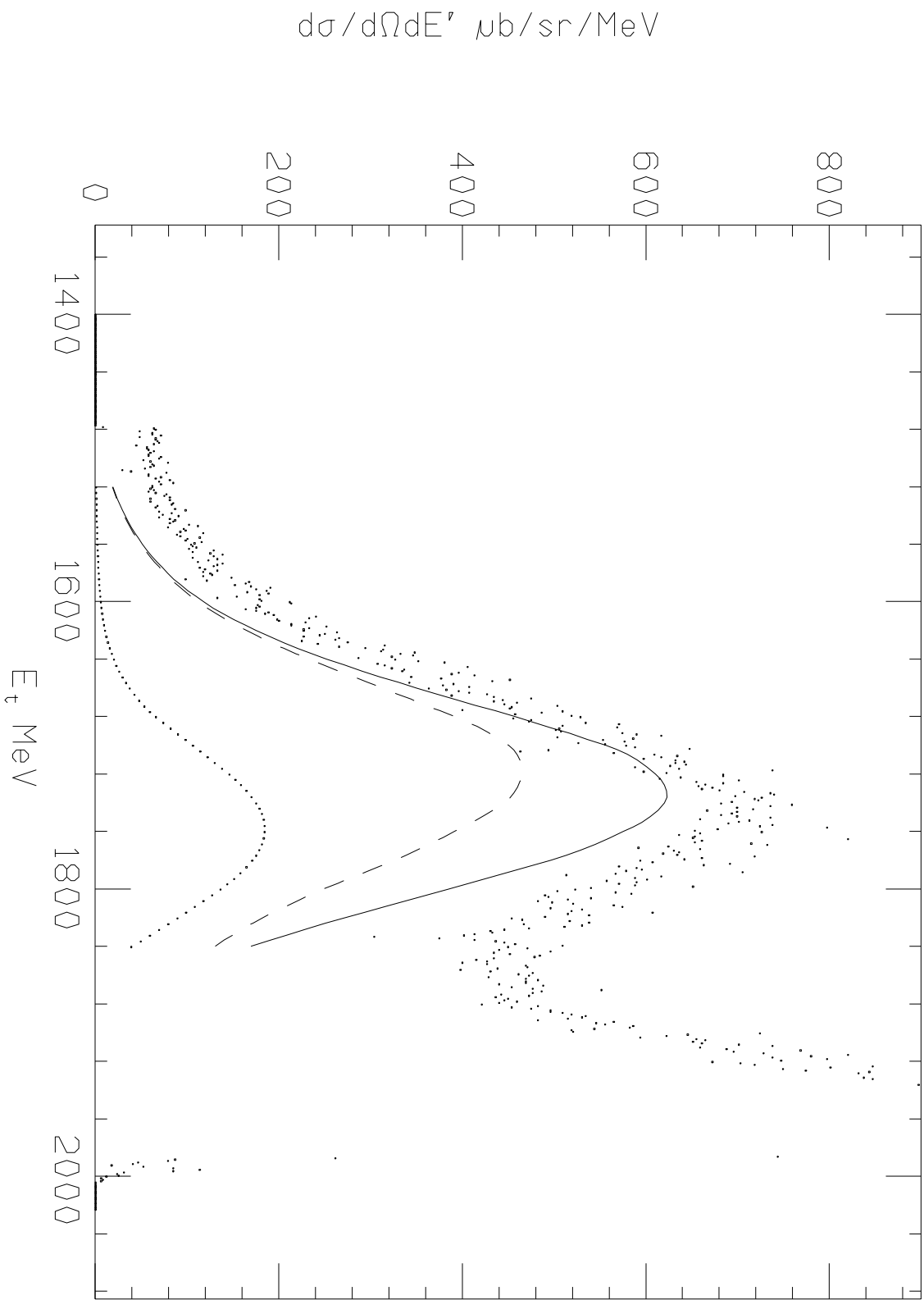


Fig. 8

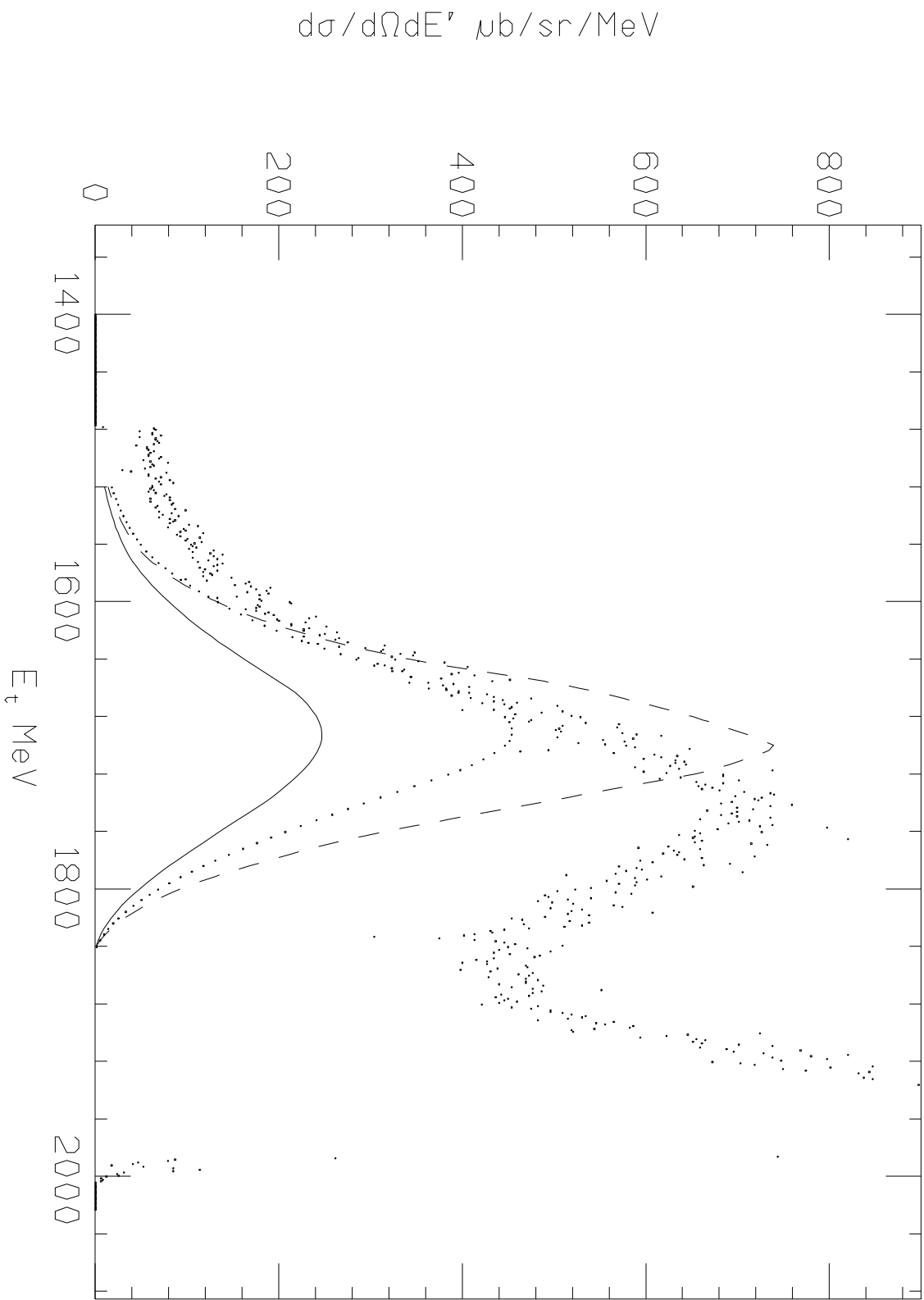


Fig. 3

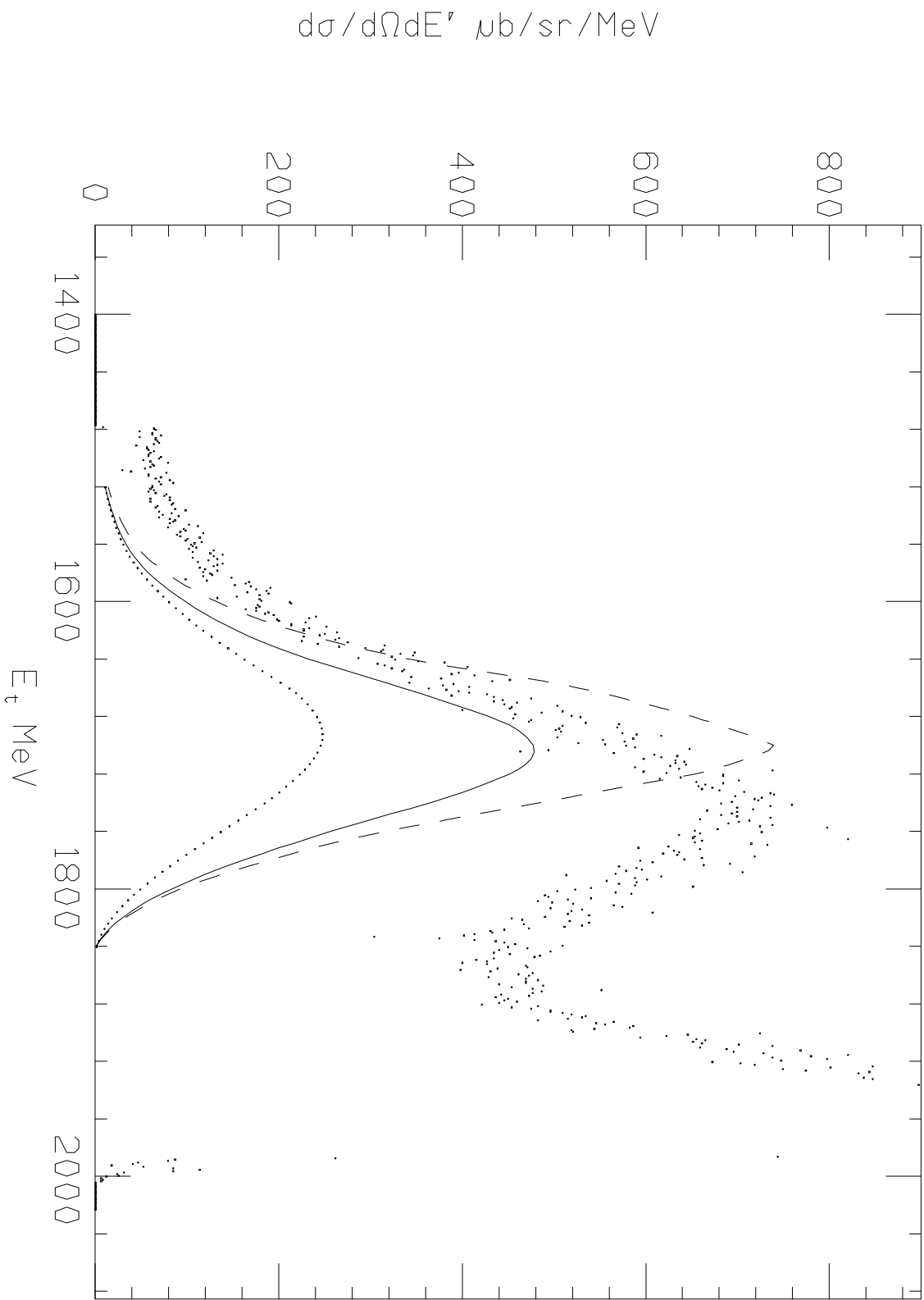


Fig. 4

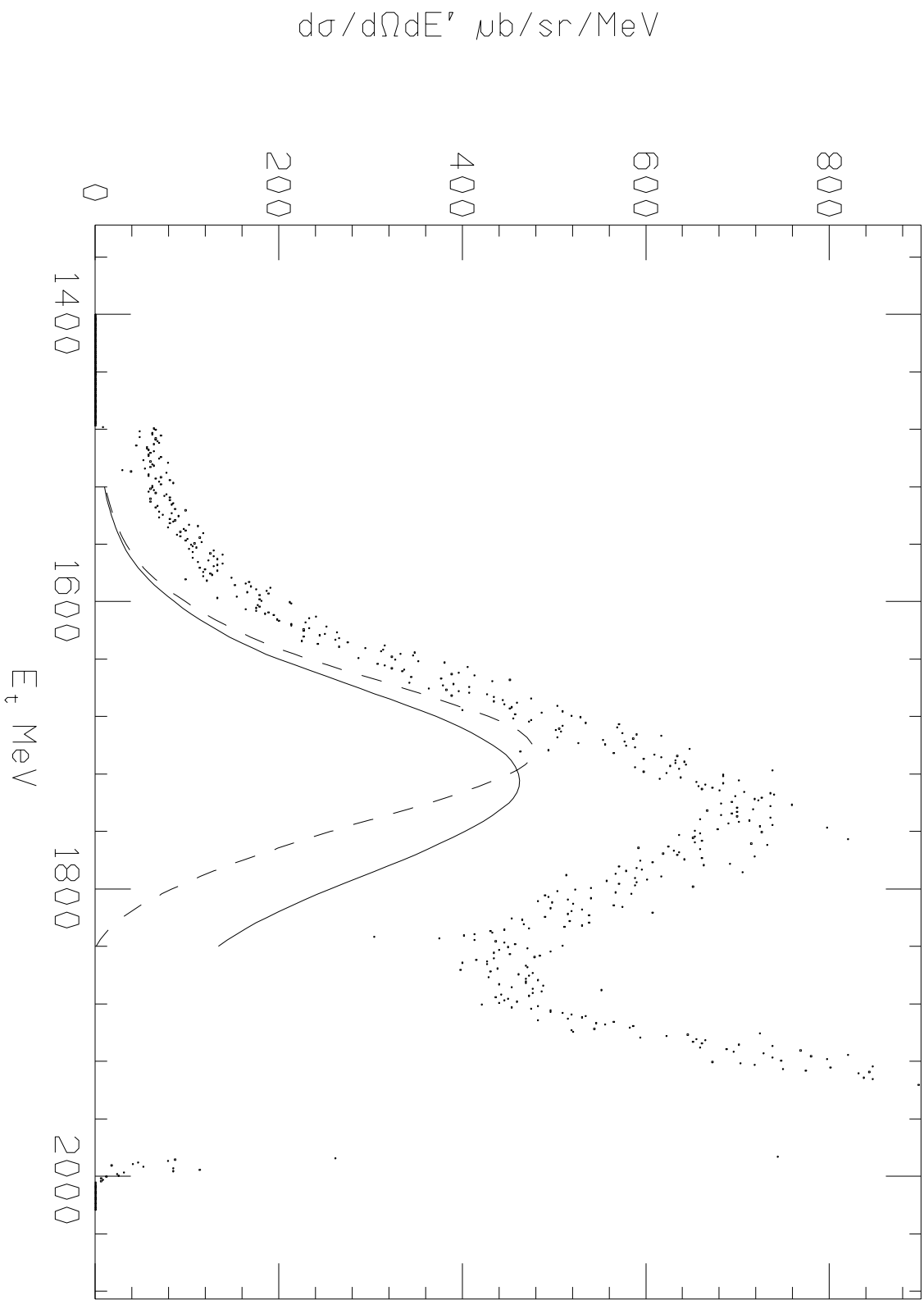


Fig. 6

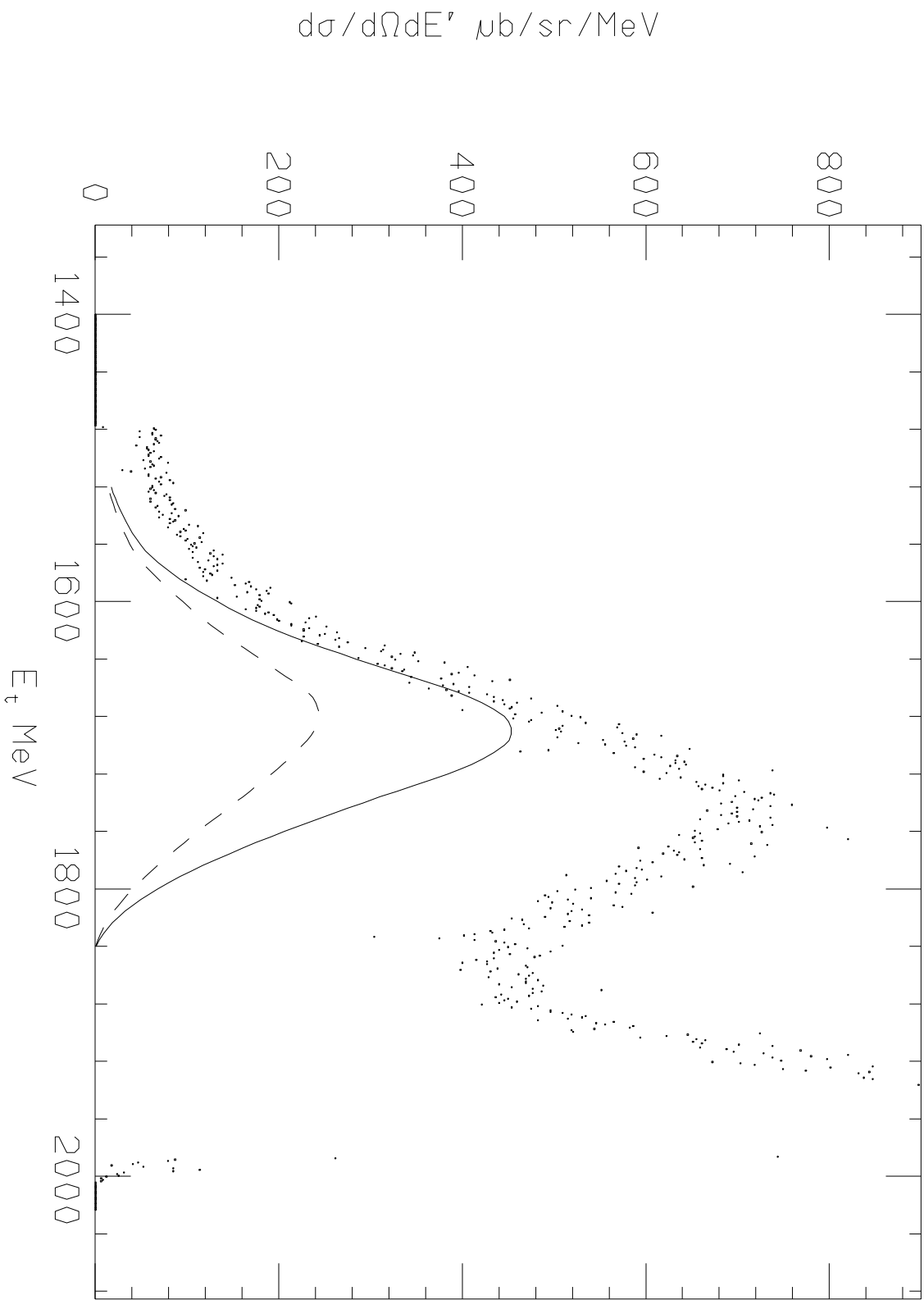


Fig. 2

$d\sigma/d\Omega dE'$ $\mu\text{b}/\text{sr}/\text{MeV}$

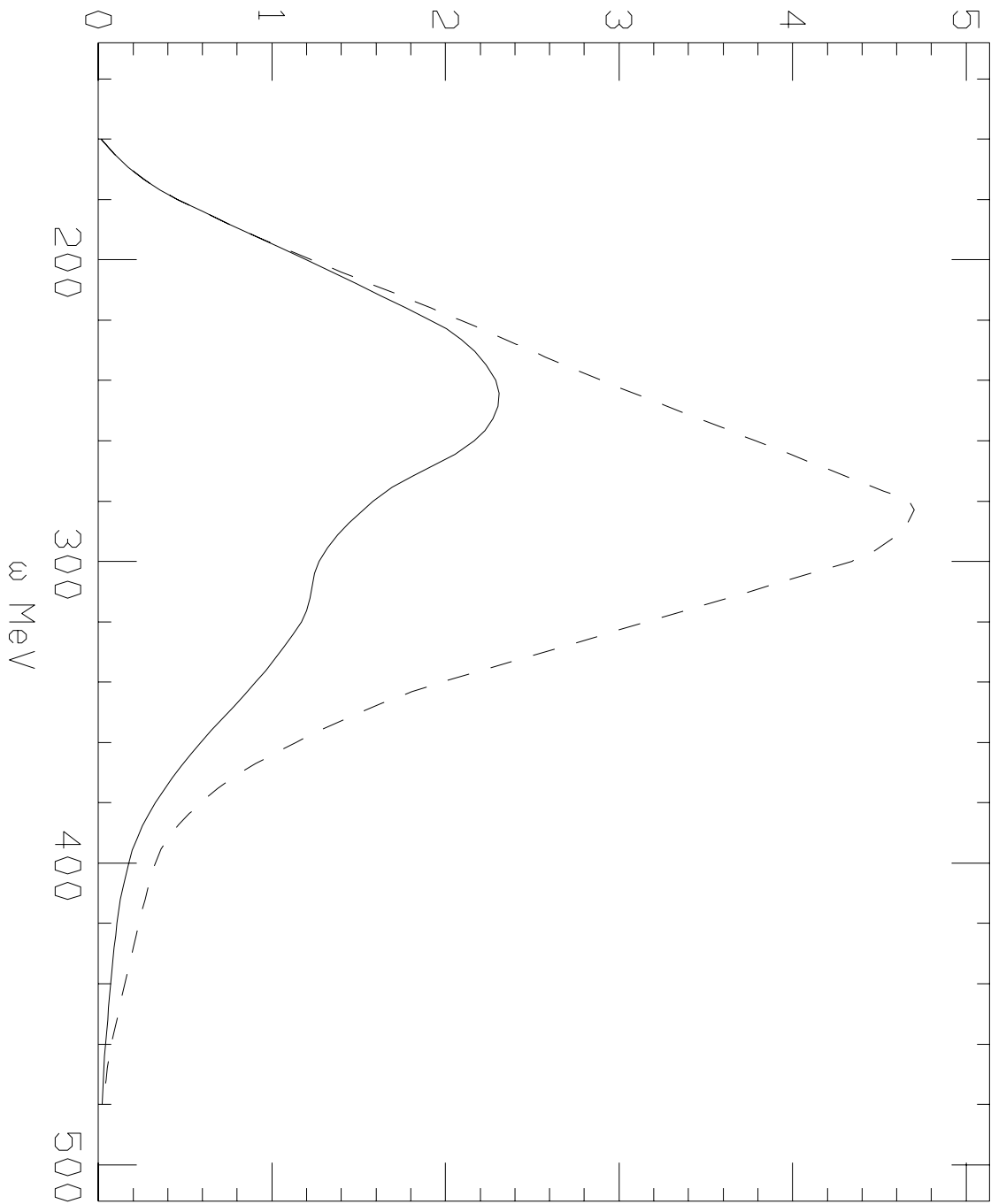


Fig. 5

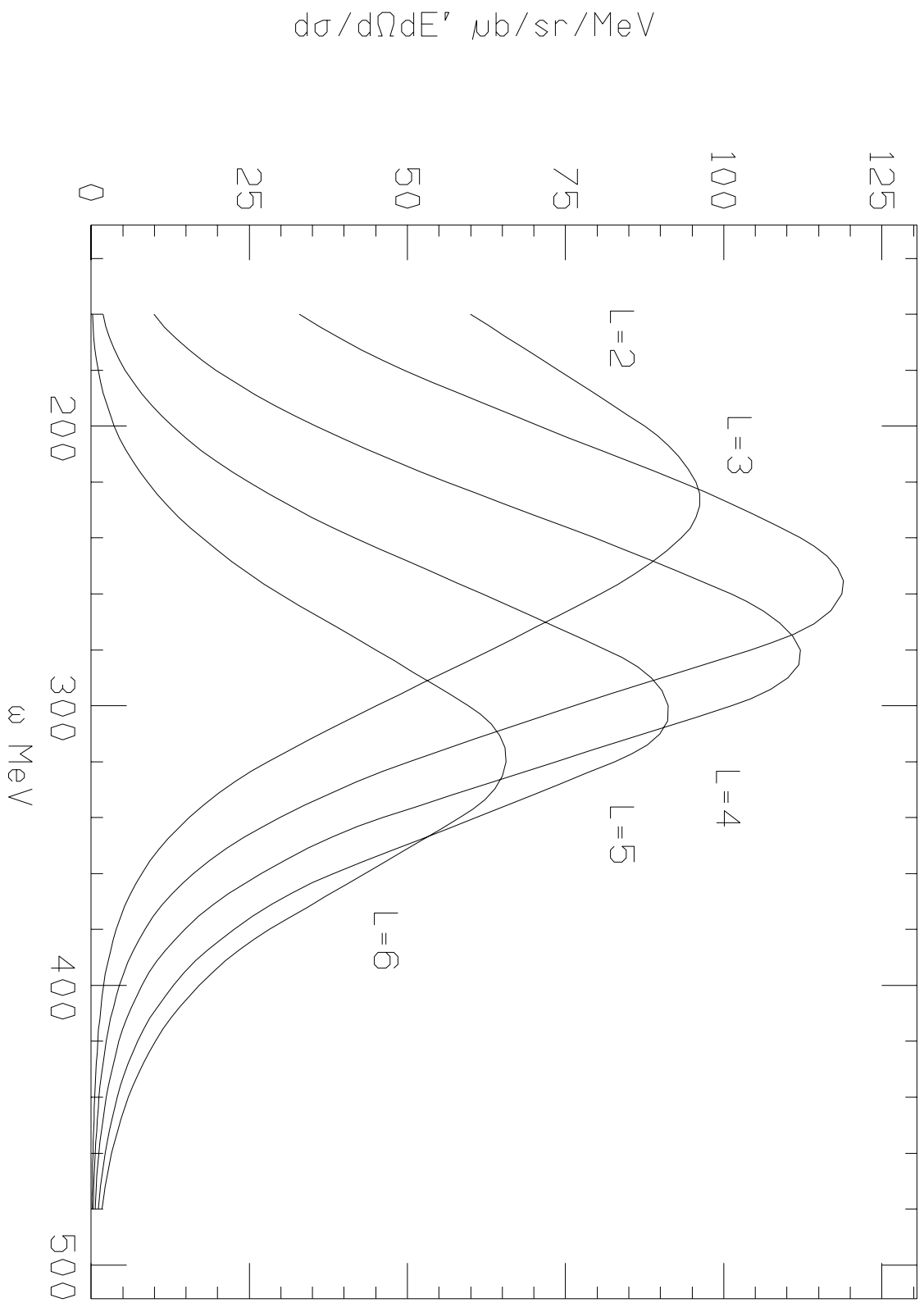


Fig. 7